metals

MDPI

Article

Extraction of Tantalum Powder via the Magnesium Reduction of Tantalum Pentoxide

Seon-Min Hwang [1], Jei-Pil Wang [2,*] and Dong-Won Lee [1,*]

[1] Titanium Department, Korea Institute of Materials Science (KIMS), Changwon, Gyeongnam 641-010, Korea; seonmin@kims.re.kr

[2] Department of Metallurgical Engineering, Pukyoung National University, Busan 48513, Korea

* Correspondence: ldw1623@kims.re.kr (D.-W.L.); jpwang@pknu.ac.kr (J.-P.W.); Tel.: +82-55-280-3524 (D.-W.L.); +82-51-629-6341 (J.-P.W.)

Received: 22 December 2018; Accepted: 4 February 2019; Published: 9 February 2019

Abstract: The metallic tantalum powder was successfully synthesized via reduction of tantalum pentoxide (Ta_2O_5) with magnesium gas at 1073~1223 K for 10 h inside the chamber held under an argon atmosphere. The powder obtained after reduction shows the Ta–MgO mixed structure and that the MgO component was dissolved and removed fully via stirring in a water-based HCl solution. The particle size in the tantalum powder obtained after acid leaching was shown to be in a range of 50~300 nm, and the mean internal crystallite sizes measured by the Scherrer equation varied from 11.5 to 24.7 nm according to the increase in reduction temperatures. The temperature satisfactory for a maximal reduction effect was found to be 1173 K because the oxygen content was minimally saturated to about 1.3 wt %.

Keywords: tantalum powder; magnesium reduction; Ta_2O_5 powder; MgO; HCl solution

1. Introduction

Tantalum is one of the key rare metals that has an extremely high melting temperature of 3290 K. Due to the excellent elasticity and corrosion resistance, it has been actively used as an alloying element into a super-alloy applied in the military parts such as jet engine, missile, and so on [1–3]. Additionally, the dielectric properties of the anodic oxide have allowed for its application as a raw material in the production of capacitors in the electronic industry [4]. Therefore, many studies have been done to secure high-purity tantalum material.

Generally, pure metals are extracted via reduction of their oxide phase with a reductant media such as hydrogen or carbon [5]. In the case of tantalum metal, tantalum pentoxide (Ta_2O_5) has been regarded as an initial material, but its reduction is nearly impossible, practically and theoretically, by hydrogen gas, by vacuum, or by carbon due to its high thermodynamic stability.

Conventionally, metallic tantalum powder is produced via reaction of tantalum pentoxide (Ta_2O_5) as a raw material, hydrofluoric acid (HF) and potassium fluoride (KF) as catalysts, and sodium as a reductant [6]. However, it has been considered that such reducing agents are considerably harmful. Several works have been found in fields using special reducers such as aluminum, magnesium, and silicon [7–10]. Among them, calcium is risky at an enhanced temperature. Applying aluminum has made it difficult to remove the aluminum oxide formed after reduction. Molten aluminum or calcium is usually used as a reductant [11]. When using magnesium, we found that 1) the reduction temperature is relatively low, 2) handling is relatively easier, and 3), after reduction via magnesium, the magnesium oxide (MgO) of a by-product can be easily eliminated by acid leaching. On the other hand, the main drawback in magnesiothermic reduction is the considerable consumption of magnesium by vaporization; moreover, the precise and careful removal of fine metallic magnesium particles

condensed on the surface of the inner reactor is required. To avoid such difficulty, self-propagating high-temperature synthesis (SHS) has been studied with preform compacted with magnesium powder [12–14]. In spite of the above-mentioned drawbacks, many works on magnesiothermic gas reduction from tantalum oxide to tantalum have been done. However, multiple oxides, such as $MgTa_2O_6$ and $Mg_4Ta_2O_9$, have been employed as raw materials to produce nanosized tantalum powder [15,16]. Scrap recycling, the flux effect, and so on have been studied with fixed reduction temperatures [8,17,18]. In this study, we investigated the reduction behavior from pure tantalum oxide to tantalum powder via magnesium gas with various reduction temperatures and studied the characterizations of product powders, such as the phase evaluation and microstructure.

2. Experiment Methods

For the magnesium reduction, we used tantalum pentoxide powder (99.99%) and pure magnesium (99.9%) purchased from Jiujiang Ltd. (Jiujiang, China) as raw materials. The reactors for the reduction were made of stainless steel, and the framework of the reactor inside for inserting raw material and magnesium is represented in Figure 1. Twenty grams of tantalum oxide powder was inserted, and the amount of magnesium needed to reduce it fully was 5.4 g theoretically. However, because magnesium not only reacts with Ta_2O_5 but can also be consumed by condensation on the surface of the inner wall of the upper reactor, 10 g of excess magnesium was prepared.

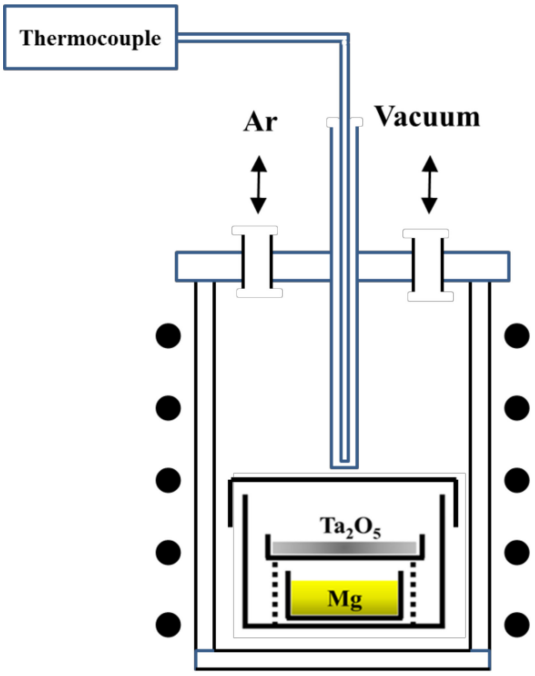

Figure 1. Schematic structure of the reactor for Mg reduction of Ta_2O_5 powder.

After repetitively treating the reactor with a vacuum and argon gas atmosphere and filling it to 1.5 atm of argon gas, it was heated at a rate of 10 K/min to 1073 K, 1123 K, 1173 K, and 1223 K for reduction reactions, respectively. The reduction time was fixed to 10 h, and the argon atmosphere was held for a full period until it was cooled to room temperature. The reduction reaction took place with magnesium gas that was evaporated from liquefied magnesium and tantalum oxide. The magnesium oxide formed after the reduction was removed by chemical washing with stirring and a filtering technique in a 5% hydrochloric acid solution. Tantalum metal powders were then obtained. We characterized the microstructure, phase evaluation, and chemical compositions with a scanning electron microscope (MIRA3 LM) (TESCAN, Brno, Czech Republic), an X-ray diffractometer

(D/Max 2500) (Rigaku, Tokyo, Japan), and an oxygen–nitrogen analyzer (ELTRA ON-900) (ELTRA, Haan, Germany).

3. Result and Discussion

The reduction occurred in the reaction via magnesium gas and tantalum oxide, and resulted in the formation of a secondary product, magnesium oxide, inside which reduced metallic tantalum powder may have existed. The reason why this reaction is possible can be explained by the fact that the thermodynamic stability of magnesium oxide is much higher than that of tantalum oxide.

Figure 2 is the SEM microstructure of the raw material powder and the tantalum pentoxide, whose overall-round shape shows an agglomerated morphology. Its size was in the range of about 200–500 nm. X-ray diffraction was studied for phase evaluation, and the result is represented in Figure 3.

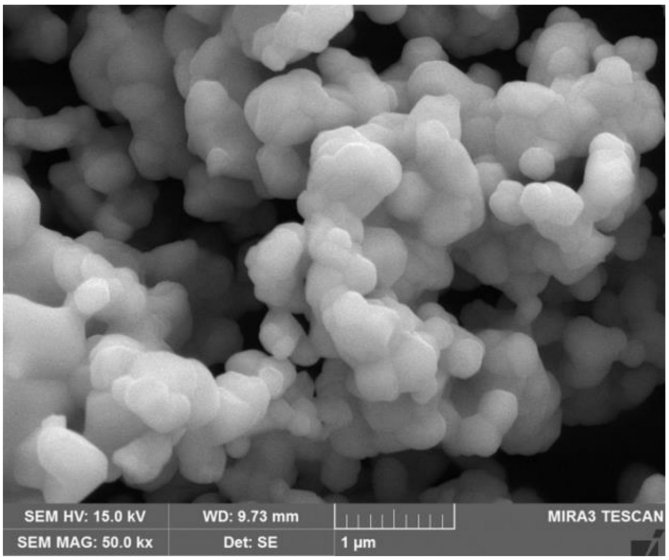

Figure 2. SEM microstructure of raw Ta_2O_5 powder.

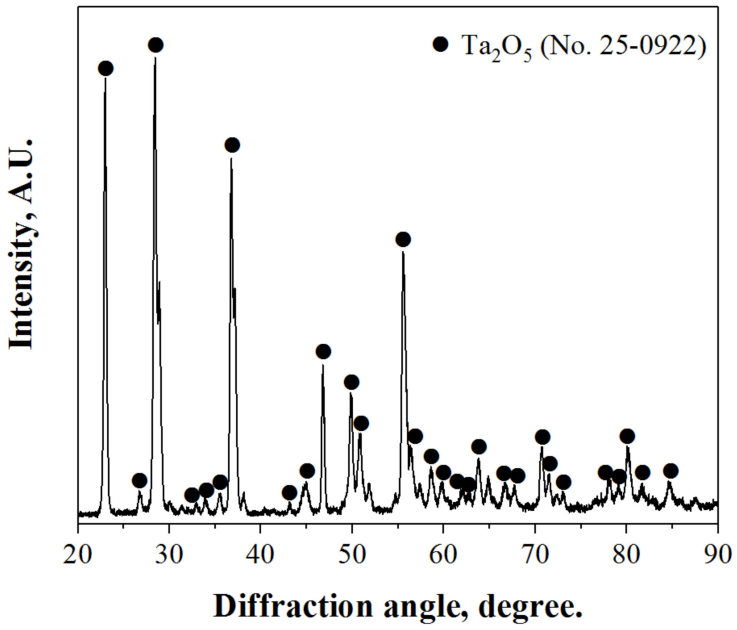

Figure 3. X-ray diffraction patterns measured in the raw Ta_2O_5 powder.

The equilibrium phase diagram of magnesium and tantalum in Figure 4 was studied using thermochemical software (FactSage 7.2, collaborative between THERMFACT/CRCT (Montreal, QC, Canada) and GTT-Technologies (Aachen, Germany) [19]. We found no mutual solubility between magnesium gas and metal tantalum in the region of temperature reduction. Therefore, the magnesium gas, a reducing agent, only reduced the oxygen component in the tantalum oxide and did not alloy with metal tantalum. Therefore, because it is possible to remove only the components of the formed magnesium oxide and the unreacted magnesium mixed with the product, metallic tantalum powder could be effectively obtained.

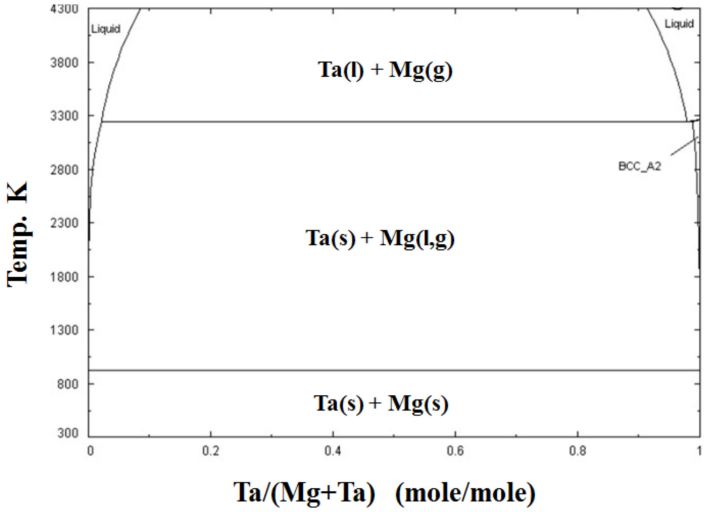

Figure 4. Ta–Mg phase diagram.

As shown in Equation (1) below, the change in the free energy obtained by HSC-5.1 software about magnesium reduction reaction in the area of 1073~1223 K is about –900 kJ/mole, which shows that the driving force for reaction is tremendous.

$$Ta_2O_5(s) + 5Mg(g) = 2Ta(s) + 5MgO(s) \quad \Delta G_{1073\ K\ \sim 1223\ K} = -987 \sim -891\ kJ/mole \tag{1}$$

The reduction behavior can be explained by the relation of the diffusion pass of oxygen. That is, as shown in Figure 5, the Mg reduction of tantalum oxide started from the powder surface via magnesium gas and led to the formation of a film of magnesium oxide. By a continuous reaction with magnesium gas existing outside, the oxygen component inside the particles was diffused out in the direction of $Ta_2O_5 \rightarrow Ta_2O \rightarrow Ta$ while the reduction reaction was processed. The reason why the reduction was processed with the formation of Ta_2O is based on the confirmation of the existence of an insufficiently reduced phase, Ta_2O, as shown in Figure 10.

After the reduction reaction was finished, metal tantalum powder may have existed inside the powder and the magnesium oxide formed on the surface. Since the formed magnesium oxide components can be fully removed via agitating and washing in weak hydrochloric acid, pure metal tantalum powders were gained. The changes in Gibbs free energy of the reaction where magnesium oxide was washed and removed in a hydrochloric acid solution can be expressed in the following equations:

$$Mg + 2HCl = MgCl_2 + H_2 \quad \Delta G_{298K} = -401\ kJ/mole \tag{2}$$

$$MgO + 2HCl = MgCl_2 + H_2O \quad \Delta G_{298K} = -61\ kJ/mole \tag{3}$$

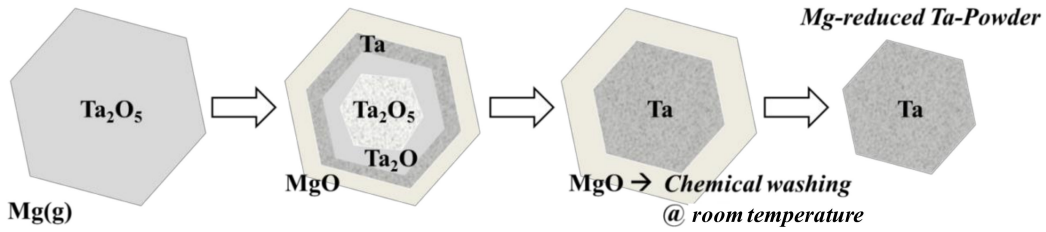

Figure 5. Schematic concept of the reduction behavior from Ta_2O_5 to Ta via magnesium gas.

Figures 6 and 7 represent the X-ray diffraction profile and SEM microstructure studied in the powder reduced at 1173 K, that is, before removing the magnesium oxide. The two phases of tantalum and magnesium oxide without tantalum oxides shown in Figure 6 indicate that the reduction reaction was well processed.

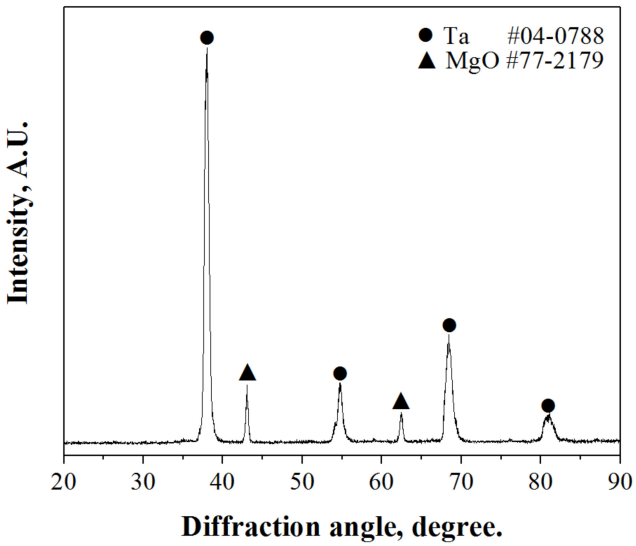

Figure 6. X-ray diffraction patterns measured in the Mg-reduced sample at 1173 K before acid leaching.

In the SEM microstructure (Figure 7), the particles are hundreds of nanometers in size and appear to be in an absorbed state by small particles with dozens of nanometers. These absorbed particles were estimated to be particles of magnesium oxide formed by the reduction, and this formation is found in reduction process.

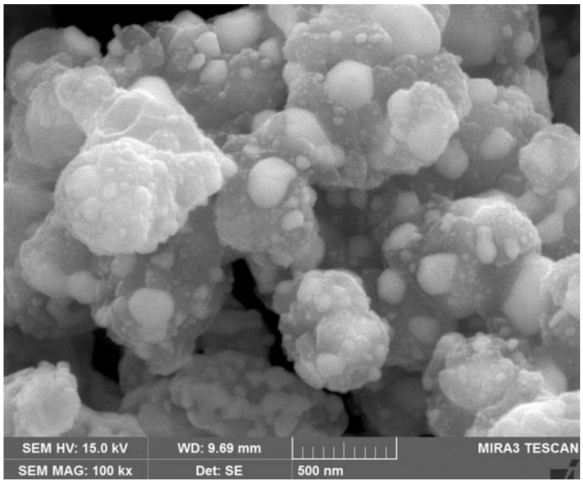

Figure 7. SEM microstructure of the Mg-reduced powder at 1173 K before acid leaching.

Figure 8 is the SEM microstructures of the pure tantalum powder obtained after reduction at 1073 K and 1173 K after acid leaching. Overall, the particles have a finer morphology than those of the raw material shown in Figure 2, particularly if the sample is at less than 1073 K. The formation of such fine structures can be explained by the restraint effect of the growth of tantalum nuclei because the reduction temperature is much lower than the melting point of tantalum metal.

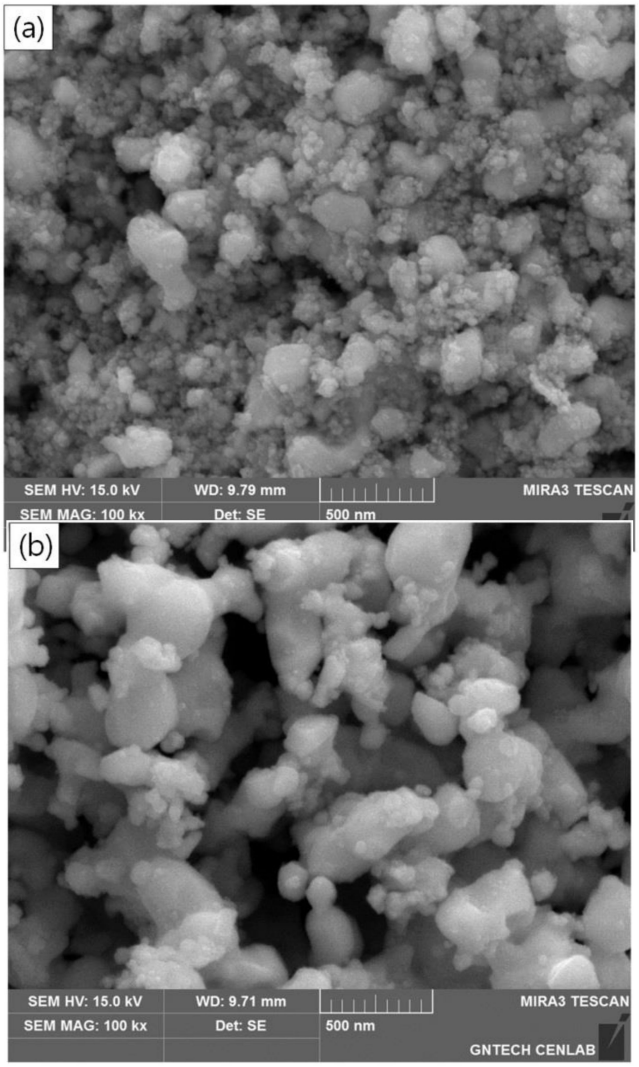

Figure 8. SEM microstructure of the Mg-reduced sample at (**a**) 1073 K and (**b**) 1173 K after acid leaching.

There is a possibility that the relatively coarse particles shown in Figure 8 are poly-crystallite and are not single-crystallite. Therefore, we measured the size of the internal crystallites by using the Scherrer equation ($B = K\lambda/D{\cdot}\cos\theta_B$) [20], and the result is shown in Figure 9.

The Scherrer equation was applied to the 1st peak in the XRD profiles. B is the full width at half maximum, HWHM (radian) is the diffraction peak, λ is the wavelength of the radiation (nm), θ_B is the Bragg angle, and D is the crystallite size (nm), respectively. Figure 9 indicates that the average crystalline sizes were increased within a range of 11.5~24.7 nm according to an increase in reduction temperatures, and this was considered to be a crystal growth effect.

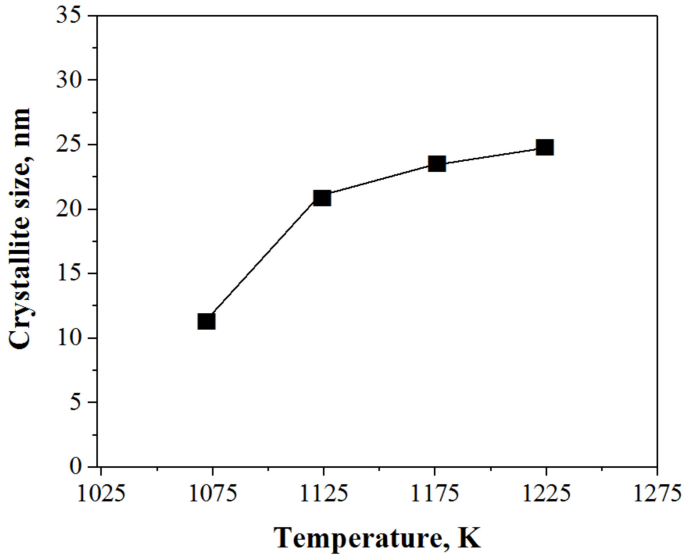

Figure 9. Crystallite sizes obtained by the Scherrer method in Mg-reduced tantalum powder.

In the next step, we compared all X-ray profiles diffracted in powders produced at various reduction temperatures, and this result is shown in Figure 10. The insufficiently reduced phase, Ta_2O, shown in Figure 5 was shown in the samples at relatively low reduction temperatures. Temperatures over 1173 K indicated a clear tantalum peak. Such insufficient reductions at lower temperatures resulted from the effect of a lower reduction driving force and the partial pressure of magnesium gas.

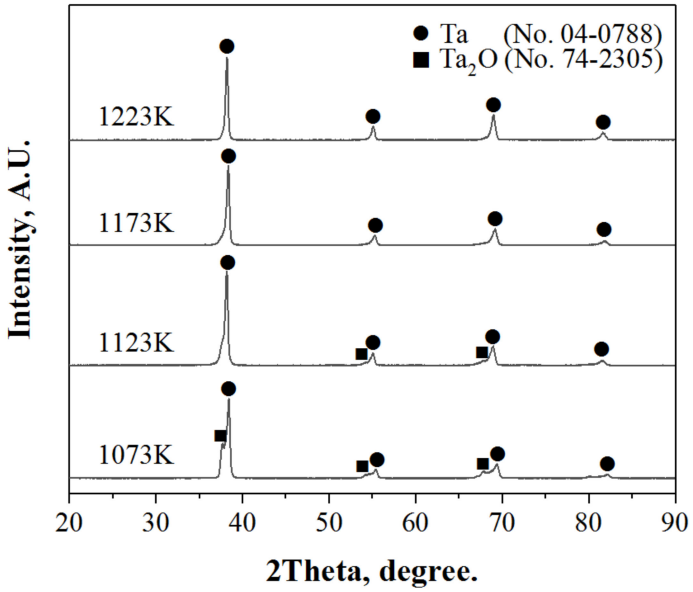

Figure 10. X-ray diffraction patterns measured in Mg-reduced samples at various reduction temperatures.

The oxygen content of the tantalum metal powder obtained from each reduction was analyzed quantitatively (Table 1). The oxygen content of the reduced powder at 1073 K was very high, 11.57 wt %, and decreased gradually to 1.25 wt % with the increase in reduction temperature. The oxygen content in the tantalum powder may have originated from inner oxygen components in the tantalum particles and the passive film formed on the surface. Therefore, the oxygen in the samples at 1173 K and 1223 K, where the reductions were well formed, was mainly detected in the passive surface film. On the contrary, in the samples insufficiently reduced at 1073 K and 1123 K, the oxygen may have come from both inside the powder and from the passive film. However, we insist the oxygen came from the

passive film because the particles produced at low temperature were significantly fine (Figure 8a), which caused high specific surface areas (Table 1). Turning to the samples at 1173 K and 1223 K, it was shown that the detected oxygen content was not much different. We concluded that the reduction temperature of 1173 K is a more satisfactory condition in view of thermal energy saving.

Table 1. Oxygen content (wt %) and specific surface area (m^2/g) measured in Mg-reduced tantalum powder at different temperatures.

Temp., K	1073	1123	1173	1223
O, wt %	11.57	6.46	1.35	1.25
S, m^2/g	21.81	12.23	7.11	6.52

4. Conclusion

Pure tantalum powder was successfully produced via magnesium reduction with tantalum pentoxide as a raw material. The structure of the powder after Mg reduction was in an agglomerated form of tiny particles of dozens of nm absorbed on the surface of coarse particles. After removing the magnesium oxide component in a hydrochloric acid solution, tantalum powder was transfigured to a structure with a range of particle sizes, approximately 50~300 nm, finer than the particle sizes of raw powder. The reduction reaction occurred via Ta_2O in an intermediate phase.

As a result of X-ray analysis in tantalum metal powders obtained by various reduction temperatures, full reduction occurred at over 1173 K. The oxygen content of the produced powder was shown then to be in a minimal range of 1.25~1.35 wt %. The average crystalline size in powders, determined by the Scherrer equation, increased from 11.5 to 24.7 nm with the increase in reduction temperature.

Author Contributions: Writing—original draft preparation, S.M.H. and D.W.L.; writing—review and editing, J.P.W.

Funding: This research received no external funding.

Conflicts of Interest: The authors declare no conflict of interest.

References

1. Cardonne, S.M.; Kumar, P.; Michaluk, C.A.; Schwartz, H.D. Tantalum and its Alloys. *Int. J. Refract. Met. Hard Mater.* **1995**, *13*, 187–191. [CrossRef]
2. Won, H.I.; Nersisyan, H.H.; Won, C.W. Combustion synthesis-derived tantalum powder for solid-electrolyte capacitor. *J. Alloys Compd.* **2009**, *478*, 716–720. [CrossRef]
3. Han, F.F.; Chang, J.X.; Li, H.; Lou, L.H.; Zhang, J. Influence of Ta content on hot corrosion behavior of a directionally solidified nickel base superalloy. *J. Alloys Compd.* **2015**, *619*, 102–108. [CrossRef]
4. Korinek, G.J. Tantalum in Solid Electrolytic Capacitors-New Developments. *Mater. Trans.* **1996**, *37*, 1244–1246. [CrossRef]
5. Loveleen, B.K.; Gourav, S.; Navjot, K.; Pandey, O.P. Thermal stability and structural properties of Ta nanopowder synthesized via simultaneous reduction of Ta_2O_5 by hydrogen and carbon. *J. Therm. Anal. Calorim.* **2015**, *119*, 175–182.
6. Kolosov, V.N.; Orlov, V.M.; Miroshnichenko, M.N.; Prokhorova, T.Yu. Preparation of Tantalum Powders via the Sodium Reduction of Potassium Heptafluorotantalate Heat-Treated in Air. *Inorg. Mater.* **2015**, *51*, 116–121. [CrossRef]
7. Brito, R.A. de.; Medeiros, F.F.P.; Gomes, U.U.; Costa, F.A.; Silva, A.G.P.; Alves Jr, C. Production of tantalum by aluminothermic reduction in plasma reactor. *Refract. Met. Hard Mater.* **2008**, *26*, 433–437. [CrossRef]
8. Okabe, T.H.; Sato, N.; Mitsuda, Y.; Ono, S. Production of Tantalum Powder by Magnesiothermic Reduction of Feed Preform. *Mater. Trans.* **2003**, *44*, 2646–2653. [CrossRef]
9. Awasthi, A.; Bhatt, Y.J.; Krishnamurthy, N.; Ueda, Y.; Garg, S.P. The reduction of niobium and tantalum pentoxides by silicon in vacuum. *J. Alloys Compd.* **2001**, *315*, 187–192. [CrossRef]

10. Purushotham, Y.; Ravindranath, K.; Kumar, A.; Govindaiah, R.; Prakash, T.L. Quality improvements in tantalum powder by automation of sodium. *Inter. J. Refract. Met. Hard Mater.* **2009**, *27*, 571–576.
11. Munter, R.; Parshin, A.; Yamshchikov, L.; Plotnikov, V.; Gorkunov, V.; Kober, V. Reduction of tantalum pentoxide with aluminium and calcium: Thermodynamic modeling and scale skilled test. *Proc. Est. Acad. Sci.* **2010**, *59*, 243–252. [CrossRef]
12. Nersisyan, H.H.; Lee, J.H.; Lee, S.I.; Won, C.W. The role of the reaction medium in the self propagating high temperature synthesis of nanosized tantalum powder. *Combust. Flame.* **2003**, *135*, 539–545. [CrossRef]
13. Orlov, V.M.; Kryzhanov, M.V. Magnesium-Thermic Reduction of Tantalum Oxide by Self-propagating High-Temperature Synthesis. *Russ. Metall.* **2010**, *2010*, 384–388. [CrossRef]
14. Orlov, V.M.; Kryzhanov, M.V. Deoxidation of the Tantalum Powder Produced by Self-Propagating High-Temperature Synthesis. *Russ. Metall.* **2014**, *2014*, 191–194. [CrossRef]
15. Orlov, V.M.; Kryzhanov, M.V. Production of Tantalum Powders by the Magnesium Reduction of Tantalates. *Russ. Metall.* **2015**, *2015*, 590–593. [CrossRef]
16. Orlov, V.M.; Kryzhanov, M.V.; Kalinnikov, V.T. Magnesium Reduction of Tantalum Oxide Compounds. *Dokl. Chem.* **2014**, *457*, 160–163. [CrossRef]
17. Mineta, K.; Okabe, T.H. Development of a recycling process for tantalum from capacitor scraps. *J. Phys. Chem. Solids.* **2005**, *66*, 318–321. [CrossRef]
18. Muller, R.; Bobeth, M.; Brumm, H.; Gille, G.; Pompe, W.; Thomas, J. Kinetics of nanoscale structure development during Mg-vapour reduction of tantalum oxide. *Int. J. Mater. Res.* **2007**, *98*, 1138–1145. [CrossRef]
19. Collection of Phase Diagrams. Available online: http://www.crct.polymtl.ca/fact/phase_diagram.php?file=Mg-Ta.jpg&dir=FTlite (accessed on 9 February 2019).
20. Miranda, M.A.R.; Sasaki, J.M. The limit of application of the Scherrer equation. *Acta Crystallogr. Sect. A* **2018**, *74*, 54–65. [CrossRef] [PubMed]